JACS
JOURNAL OF THE AMERICAN CHEMICAL SOCIETY

pubs.acs.org/JACS

Article

3D Cage COFs: A Dynamic Three-Dimensional Covalent Organic Framework with High-Connectivity Organic Cage Nodes

Qiang Zhu, Xue Wang, Rob Clowes, Peng Cui, Linjiang Chen,* Marc A. Little,* and Andrew I. Cooper*

Cite This: *J. Am. Chem. Soc.* 2020, 142, 16842−16848

Read Online

ACCESS | Metrics & More | Article Recommendations | Supporting Information

ABSTRACT: Three-dimensional (3D) covalent organic frameworks (COFs) are rare because there is a limited choice of organic building blocks that offer multiple reactive sites in a polyhedral geometry. Here, we synthesized an organic cage molecule (**Cage-6-NH$_2$**) that was used as a triangular prism node to yield the first cage-based 3D COF, **3D-CageCOF-1**. This COF adopts an unreported 2-fold interpenetrated **acs** topology and exhibits reversible dynamic behavior, switching between a small-pore (**sp**) structure and a large-pore (**lp**) structure. It also shows high CO_2 uptake and captures water at low humidity (<40%). This demonstrates the potential for expanding the structural complexity of 3D COFs by using organic cages as the building units.

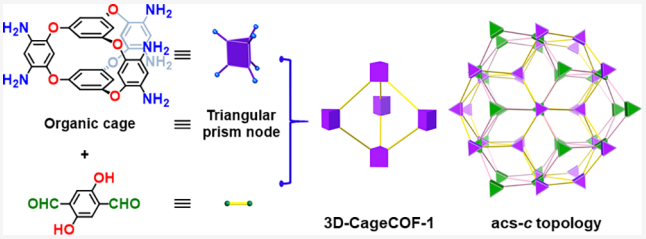

INTRODUCTION

Covalent organic frameworks (COFs) have emerged as a versatile class of crystalline porous solids that can be rationally designed and fine-tuned by synthesis to enhance their functionality.[1−4] The framework topology of a COF is predetermined by the connectivity and geometry of the building blocks, and, as for metal−organic frameworks (MOFs),[5,6] COF synthesis is often tolerant to changes in linker size and chemical functionality. As such, different COF topologies (or nets) can be purposefully targeted by a judicious choice of building blocks.

To date, the majority of reported COFs are two-dimensional (2D) layered structures with 1D pore channels, where strong noncovalent interactions modulate the interlayer packings.[7] By contrast, COFs with 3D nets require more than one nonplanar building unit, and these have proven to be less synthetically accessible.[4,8] Consequently, only eight distinct 3D nets in the Reticular Chemistry Structure Resource (RCSR)[9] have been reported for COFs: **dia**,[10] **lon**,[11] **bor**,[2] **ctn**,[2] **pts**,[12] **rra**,[13] **srs**,[14] and **ffc**.[15] The first six of these were constructed using tetrahedral building blocks with 4 points of extension, such as tetraphenylmethane, tetraphenylsilane, adamantane, and their derivatives.[4] This is in stark contrast to endeavors that have realized topologically more complex MOF nets,[16] where metal clusters with up to 24 points of extension have been reported.[17,18] However, organic molecules rarely have a high number (>4) of reactive sites that are spatially arranged to allow for extended interconnection. This is a major reason for the difficulty in broadening the range of topologies for COFs, and it is a central challenge for expanding the functional scope of porous 3D frameworks.

As with other porous 3D solids, such as zeolites,[19] MOFs,[6,20] and porous organic polymers,[21] the interconnected pore channels in 3D COFs may provide opportunities for superior function,[22,23] such as enhanced molecular diffusivity. New functions may also be possible: for example, inserting rotatable dipolar linkers into certain framework topologies could afford COFs with a net response to electric fields.[24] Moreover, many porous 3D framework structures have been shown to exhibit structural flexibility in response to adsorption, as exemplified by breathing MOFs[25] and swellable porous polymers.[26] Such complementary and cooperative phenomena in porous solids can be beneficial in applications such as controlled drug delivery, gas capture, and size-selective catalysis.[27−29] A key step to unlocking new applications for COF materials is to increase the chemical and structural diversity—for example, by accessing new framework topologies using polyhedral organic nodes.

Organic cage molecules can be viewed as polyhedrons.[30] Moreover, the vertexes of a cage polyhedron may be functionalized to link up with another building block for framework structures[31] or to expand its connectivity (e.g., 12-arm octahedral cages[32]). Cages are therefore exciting candidates for constructing 3D COFs with highly connected topologies. However, this strategy remains largely unexplored because it is challenging to design and synthesize organic cage molecules that are compatible with reticular chemistry, shape-persistent, and stable under COF synthetic conditions, not

Received: July 17, 2020
Published: September 6, 2020

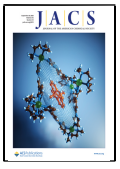

https://dx.doi.org/10.1021/jacs.0c07732
J. Am. Chem. Soc. 2020, 142, 16842−16848

least because organic cage molecules are often also assembled using dynamic covalent chemistry.[33] The first organic-cage-based COF was only recently reported, and this was a 2D net.[34] The cage molecule was used as a triangular node to connect with a linear linker, yielding the prototypical 2D **hcb** net. To the best of our knowledge, the use of organic cage molecules with higher connectivity (>3 connecting sites) to generate 3D COFs has not yet been reported.

Here, we synthesized a shape-persistent organic cage with six pendant amine groups positioned in a trigonal prismatic arrangement (**Cage-6-NH$_2$**, Figure 1). By reacting **Cage-6-NH$_2$** with the linear 2,5-dihydroxyterephthalaldehyde (DHTPA), a 3D COF, **3D-CageCOF-1**, adopting the **acs** topology was synthesized. In the extended structure of **3D-CageCOF-1**, there are two interpenetrated **acs** nets. **3D-CageCOF-1** was found to undergo reversible transformations between a small-pore (**sp**) structure and a large-pore (**lp**) structure in response to guest loading of dimethylformamide (DMF). Also, this hydrophilic **3D-CageCOF-1** exhibited a high water uptake (22 wt %) at low relative humidity (40%) and a high carbon dioxide uptake at 1 bar (204 mg/g, 273 K).

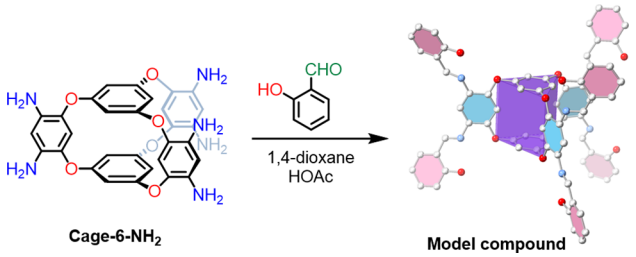

Figure 1. Synthesis of model compound and its single-crystal structure. Single-crystal atom colors: C, gray; N, blue; O, red. H atoms are omitted for clarity.

RESULTS AND DISCUSSION

The discovery of triangular prism-shaped building blocks was important for increasing the topological diversity of MOFs.[35−38] However, triangular prisms have not been used in COF synthesis because of the limited availability of suitable building blocks. To address this, we synthesized the triangular prism-shaped **Cage-6-NH$_2$** in two steps from a previously reported hexanitro precursor that was reported to have D_{3h} symmetry (Supporting Information, Schemes S1 and S2).[39] Importantly, the cage structure of **Cage-6-NH$_2$** does not contain imine or boronate ester bonds, which means that **Cage-6-NH$_2$** is compatible, in principle, with a wide range of synthetic conditions for COF formation. In addition, unlike planar molecular building blocks that usually lead to layered COFs, **Cage-6-NH$_2$** is decorated with 6 amine groups in a 3D trigonal prismatic arrangement that are ready to be extended in three dimensions.

The 3D symmetry of the amine groups in **Cage-6-NH$_2$** was initially investigated in a solution using ^{1}H and ^{13}C NMR spectroscopy (Figures S1−S4), which indicated that the cage had D_{3h} symmetry like the previously reported hexanitro precursor.[39] To investigate this further, we synthesized a model compound by reacting **Cage-6-NH$_2$** with 2-hydroxybenzaldehyde, which has a phenol group that is capable of forming hydrogen bonds with the cage molecule (Figure 1). NMR spectra of the model compound (Figures S6) again indicated that the model compound had D_{3h} symmetry in solution, and the triangular prism shape of the cage was confirmed by single-crystal X-ray structure (Figure 1 and Table S5 for refinement details). In the single-crystal structure of the model compound, the pendant amine groups were distorted away from a perfect

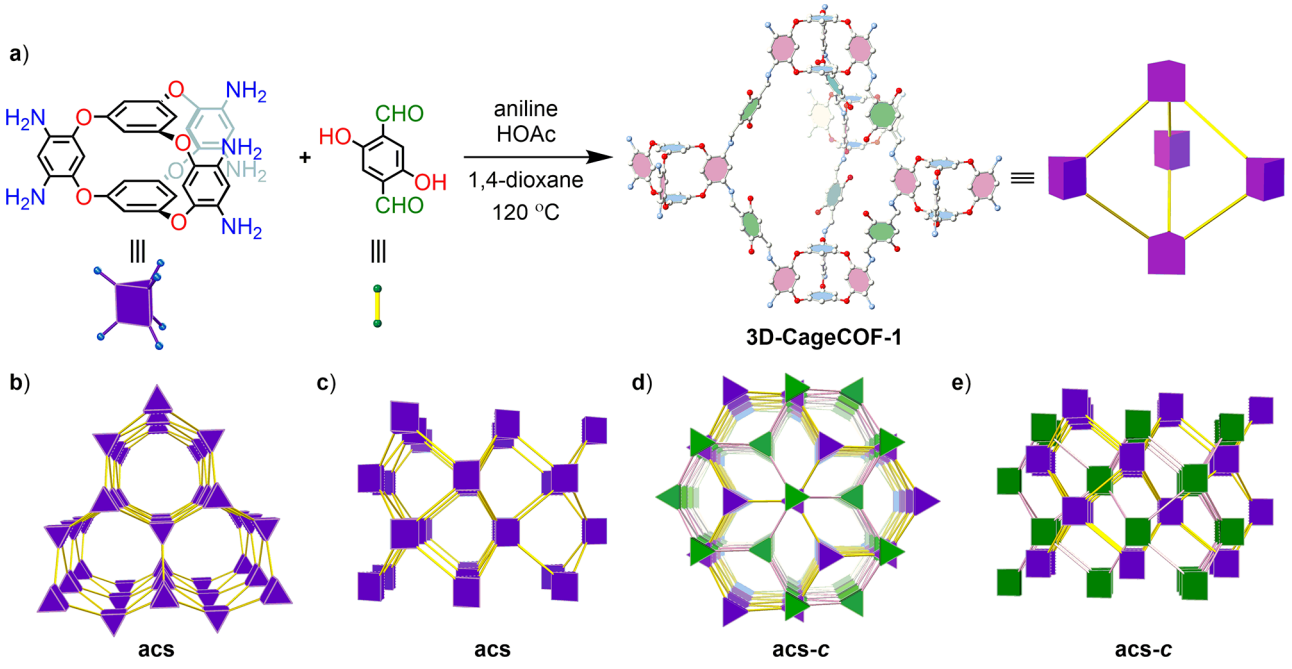

Figure 2. (a) Scheme for the synthesis of **3D-CageCOF-1** from **Cage-6-NH$_2$** and DHTPA, which can be topologically represented as a triangular prism and a linear strut, respectively. Model atom colors: C, white; N, blue; O, red. H atoms are omitted for clarity. (b, c) Two views of an **acs** crystal net, where the purple nodes represent the cage-based building blocks; (d, e) two comparable views of the 2-fold interpenetrated **acs-*c*** net (*c*, catenated), with the cage nodes belonging to the different nets colored in purple or green.

https://dx.doi.org/10.1021/jacs.0c07732
J. Am. Chem. Soc. 2020, 142, 16842−16848

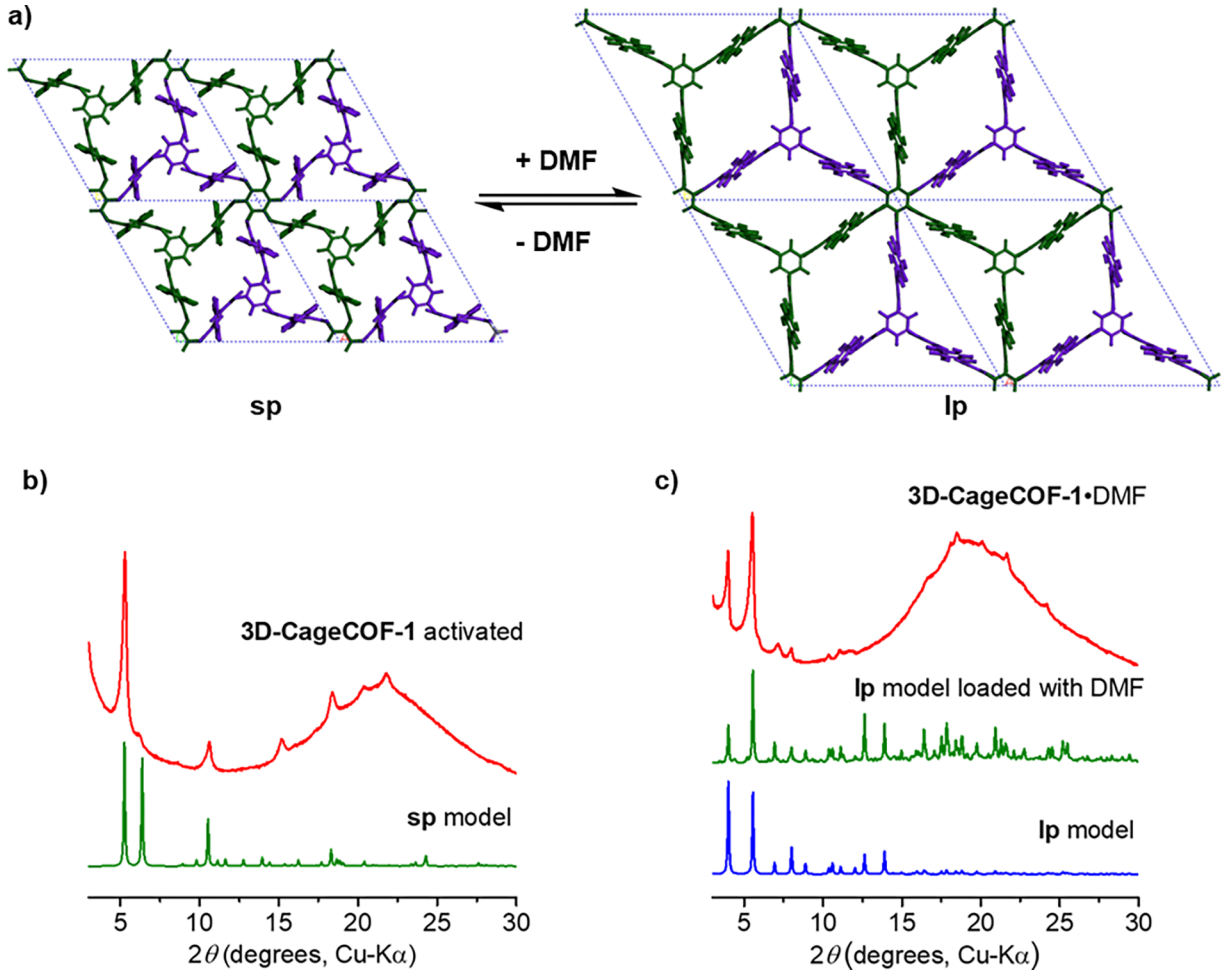

Figure 3. (a) Scheme showing the reversible structural transformation between the small-pore (**sp**) and large-pore (**lp**) forms of **3D-CageCOF-1** upon loading and the removal of DMF solvent. (b) Comparison of the experimental PXRD pattern of activated **3D-CageCOF-1** with the simulated pattern for the **sp**, 2-fold model. (c) Comparison of the experimental PXRD pattern collected on the DMF solvate of **3D-CageCOF-1** with two simulated patterns. The empty **lp** structure was optimized with the cell parameters fixed at the experimental values; the optimized **lp** structure was then loaded with DMF up to saturation at room temperature and 1 bar pressure.

trigonal prismatic geometry, although their geometry is likely to have been affected by the close packing of the pendant aromatic groups in the crystal structure (Figure S42).

The trigonal prismatic geometry of **Cage-6-NH$_2$**, along with its shape persistence in the solid state, makes it a promising candidate for constructing several 3D topologies, such as **stp**, **tpt**, **sit**, **acs**, and **nia**.[40] Here we used the combination of **Cage-6-NH$_2$** with a linear linker to target COFs with **acs** nets according to reticular chemistry.[35] DHTPA was chosen as the linear linker on the basis that intramolecular hydrogen bonds between the hydroxyl groups of DHTPA and the imine bonds in the COF product might be beneficial for directing the supramolecular assembly of the building blocks during synthesis and for stabilizing the resulting COF structure.[41] Atomistic COF models were constructed using **Cage-6-NH$_2$** and DHTPA as building blocks and the **acs** net as the blueprint (Figure 2).[42] Models of both the noninterpenetrated framework structure and its 2-fold and 3-fold interpenetrated forms were built (Figure S26). In contrast with tetrahedral-based building units, which tend to form COFs with high degrees of interpenetrations,[11,43] the bulky core of **Cage-6-NH$_2$** enables the maximum interpenetration to be limited to 3-fold, thus simplifying the task of solving the structure by simulation, assuming that an **acs** net is formed. The underlying structure of **3D-CageCOF-1** was analyzed by powder X-ray diffraction (PXRD) combined with the structural models, produced using the principles of reticular chemistry.

Despite screening several hydrothermal reaction conditions for the reaction between **Cage-6-NH$_2$** and DHTPA (Figures S7 and S8), we initially only isolated poorly crystalline samples that had weak PXRD patterns with a single peak at 5.3° (Cu-Kα; see Figures S7 and S8). The nitrogen sorption-derived Brunauer–Emmett–Teller (BET) surface areas for these poorly crystalline samples at 77 K were also low (ca. 230 m^2 g^{-1}; Figures S12 and S13). We believe that the poor crystallinity of the product was due to the poor solubilities of **Cage-6-NH$_2$** and the oligomeric byproducts in the reaction solvent, which hindered reversibility and network self-healing during the COF synthesis. Inspired by dynamic covalent chemistry-derived approaches for COF synthesis, aniline was employed as a modulator.[11] After optimizing the synthetic conditions by including 7.5 mol. equiv. of aniline per **Cage-6-NH$_2$** as a modulator and using 6 M HOAc as the catalyst, we produced a COF, **3D-CageCOF-1**, with much improved crystallinity (Figures S9–S11).

https://dx.doi.org/10.1021/jacs.0c07732
J. Am. Chem. Soc. 2020, 142, 16842–16848

The crystallinity of activated **3D-CageCOF-1** was characterized by PXRD. By treating the reflections at 2.82° and 5.65° (λ = 0.825015 Å) as the [100] and [200] reflections, respectively, in a trigonal/hexagonal symmetry structure, we were able to determine that the likely $a = b$ cell edges of the activated **3D-CageCOF-1** structure were ~19.4 Å (Figure S27), in agreement with the symmetry and cell dimensions that were calculated for the activated model with $P\bar{3}$ symmetry. Unfortunately, it was not possible to unambiguously determine the c unit cell edge from our PXRD data and, hence, to produce a meaningful fit, despite performing this measurement using synchrotron radiation (Figure S27). However, by using our structural models we were able to propose a 2-fold interpenetrated **acs-*c*** net as the most likely structure for **3D-CageCOF-1**. The noninterpenetrated structure was optimized to the $a = b$ cell length of 24.0 Å, which is much larger than the experimental values. Catenation of two such COF networks led to a significant reduction in the cell volume, owing to the strong noncovalent interactions between the two networks, thus resulting in a contracted structure referred to as a small-pore (**sp**) model in Figure 3 and hereafter. The 3-fold interpenetration also resulted in a contracted cell, similar in size to the 2-fold cell. A comparison of these simulated models with the experiment indicated that **3D-CageCOF-1** adopted an **sp**, 2-fold interpenetrated structure (Figure 3a and Figure S29).

Nitrogen sorption analysis at 77 K revealed that **3D-CageCOF-1** is microporous and has a type-II sorption isotherm (Figure S14) with a pore volume of 0.50 $cm^3\ g^{-1}$. The BET and Langmuir surface areas calculated for **3D-CageCOF-1** were 1040 and 1336 $m^2\ g^{-1}$, respectively (Figures S15 and S16). The measured BET surface area equates to 54% of the theoretical calculated nitrogen-accessible surface area for the **sp**, 2-fold model shown in Figure 3b. The pore diameters derived by fitting to the nitrogen isotherm are 8.8 and 5.6 Å, in close agreement with the pore diameters of the proposed model (8.5 and 5.1 Å; Figure S17 and Table S3 for comparison with other models). Furthermore, the simulated nitrogen adsorption isotherm uptake at 1 bar for the **sp**, 2-fold structure is also in very good agreement with the experimental counterpart (Figure S31).

Scanning electronic microscopy (SEM) indicated that activated **3D-CageCOF-1** has a flakelike morphology (Figure S32). Solid-state NMR cross-polarization magic-angle spinning (CP/MAS) confirmed the formation of imine bonds at 164 ppm (Figure S35). Thermogravimetric analysis (TGA) (Figure S36a) and differential scanning calorimetry (DSC) (Figure S36b) indicated that the COF starts to decompose at 400 °C.

Dynamic behaviors are common in 3D network materials, and this is particularly well studied and documented for MOFs.[44,45] Previous studies have also revealed that 3D COF materials can reversibly respond to stimuli, giving rise to applications in sensing[46] and adsorption.[27,47,48] Initially, to investigate the chemical stability of **3D-CageCOF-1**, we immersed powdered samples in a series of common organic solvents (MeOH, CH_3CN, tetrahydrofuran (THF), and DMF) and water for 24 h, washed the samples by Soxhlet with acetone, and then dried the samples in air. On the basis of PXRD patterns and Fourier transform infrared (FT-IR) data recorded after these experiments, we found that the structure and crystallinity of **3D-CageCOF-1** remained intact after being reactivated from these solvents (Figures S38 and S39). However, on inspection of the solvated PXRD patterns, we found that the powdered COF sample immersed in DMF solvent transformed into a new phase, **3D-CageCOF-1·DMF**, which we characterized by recording PXRD patterns on solvated samples, suspended in DMF solvent, loaded in glass capillaries (Figure 3c).

To calculate a structural model for **3D-CageCOF-1·DMF**, we initially used the DMF solvated PXRD pattern to determine potential unit cell dimensions. A close similarity was observed between the $P\bar{3}$ model and the experimental PXRD data that refined to the unit cell dimensions: $a = b$ = 25.5 Å, c = 22.9 Å, and V = 12 880 $Å^3$ (see Figure S28 for Pawley refinement (R_p = 0.8%, R_{wp} = 1.4%, and χ^2 = 2.6%)). On the basis of the experimental cell, a large-pore (**lp**), 2-fold structure was constructed and optimized, adopting the same $P\bar{3}$ symmetry. This **lp** model transformed into the **sp** model for the activated phase without fixing the unit cell parameters at the experimental values (Figure 3b; see Video 1 in the Supporting Information, which shows the **lp** model transforming into the **sp** model). Simulated PXRD patterns, using the empty or DMF-loaded **lp** structure, are in good agreement with the pattern of **3D-CageCOF-1·DMF** (Figure 3c).

3D-CageCOF-1·DMF transformed back into the activated **sp** structure after the DMF solvent molecules were thermally removed from the COF via *in situ* heating at 175 °C (Figure 40). Our structural modeling suggests that the reversible transformations between the activated **sp** and DMF-solvated **lp** phases are a result of the structure being stabilized by either the interframework interactions, leading to corrugated frameworks, or the presence of DMF solvent, allowing the frameworks to stay expanded. This flexible behavior is facilitated by a combination of the shape persistence of the cage core, the hingelike motions of the cage "arms" (oxygen-bridged phenyls), and the rotation of the imine bonds in the COF networks.

Activated **3D-CageCOF-1** has a relatively small pore size and the pores are highly decorated with oxygen and nitrogen atoms, in principle providing a favorable polar, hydrophilic environment for guests such as CO_2 and H_2O. To support this, **3D-CageCOF-1** has a maximum CO_2 uptake of 204 mg g^{-1} at 273 K and 1 bar, and 107 mg g^{-1} at 298 K and 1 bar (Figure 4a), which are among the highest values reported for COFs under these conditions (Figure S20).[49−51] **3D-CageCOF-1** also exhibits an S-shaped water vapor sorption isotherm with a small desorption hysteresis at 298 K, which is a desirable sorption behavior for water capture by nanoporous solids.[52] In

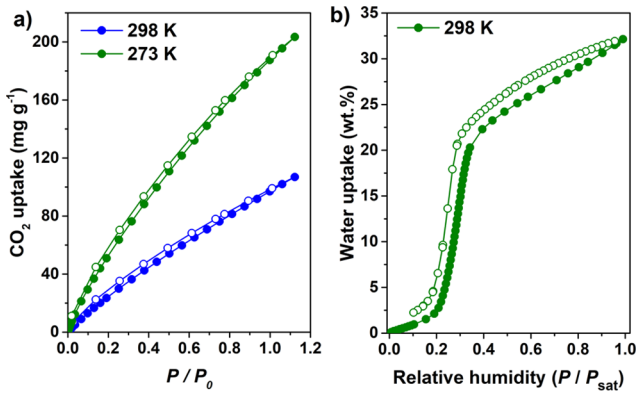

Figure 4. (a) CO_2 isotherms and (b) water vapor sorption isotherms for **3D-CageCOF-1**.

https://dx.doi.org/10.1021/jacs.0c07732
J. Am. Chem. Soc. 2020, 142, 16842−16848

addition, **3D-CageCOF-1** shows a steep pore filling in the pressure (P/P_0) range of 0.21−0.34, achieving an adsorption capacity of 22 wt % at P/P_0 = 0.4 and a maximum capacity of 33 wt % (Figure 4b); this is comparable with the best performing COF material (COF-432) reported for water harvesting.[52] Also, there was no marked loss in performance after three adsorption−desorption cycles (Figure S23), suggesting that **3D-CageCOF-1**, or analogues thereof, could be a promising candidate for water capture.

CONCLUSION

In conclusion, we have synthesized a 3D organic-cage-based COF for the first time, **3D-CageCOF-1**, which adopts the **acs** crystal net in a 2-fold interpenetrated form. Our strategy leverages a rationally designed organic cage molecule that is shape-persistent and offers six reactive sites, arranged in a triangular prism geometry, that are ready for extension in three dimensions. **3D-CageCOF-1** exhibits dynamic behavior toward DMF and shows promising performance for water harvesting and CO_2 uptake. This work affords a new strategy for expanding the library of COF building units and enriching the range of network topologies that can be accessed. It also demonstrates the potential for embedding organic cage molecules into COFs to discover new functional materials, for example, by designing cages that can impart additional functionality, such as preformed pores to bind specific guests.

ASSOCIATED CONTENT

Supporting Information

The Supporting Information is available free of charge at https://pubs.acs.org/doi/10.1021/jacs.0c07732.

Computational methodology, powder and single-crystal X-ray diffraction, SEM, TEM, DSC, TGA, and gas and vapor sorption analysis (PDF)

X-ray crystallographic data of **Cage-6-NO$_2$** (CIF)

X-ray crystallographic data of model compound (CIF)

lp model transforming into the **sp** model (MP4)

Computation models for sp and lp structures (ZIP)

AUTHOR INFORMATION

Corresponding Authors

Linjiang Chen − *Department of Chemistry and Materials Innovation Factory and Leverhulme Research Centre for Functional Materials Design, University of Liverpool, Liverpool L7 3NY, United Kingdom*; Email: lchen@liverpool.ac.uk

Marc A. Little − *Department of Chemistry and Materials Innovation Factory, University of Liverpool, Liverpool L7 3NY, United Kingdom*; orcid.org/0000-0002-1994-0591; Email: malittle@liverpool.ac.uk

Andrew I. Cooper − *Department of Chemistry and Materials Innovation Factory and Leverhulme Research Centre for Functional Materials Design, University of Liverpool, Liverpool L7 3NY, United Kingdom*; orcid.org/0000-0003-0201-1021; Email: aicooper@liverpool.ac.uk

Authors

Qiang Zhu − *Department of Chemistry and Materials Innovation Factory, University of Liverpool, Liverpool L7 3NY, United Kingdom*

Xue Wang − *Department of Chemistry and Materials Innovation Factory and Leverhulme Research Centre for Functional Materials Design, University of Liverpool, Liverpool L7 3NY, United Kingdom*

Rob Clowes − *Department of Chemistry and Materials Innovation Factory, University of Liverpool, Liverpool L7 3NY, United Kingdom*

Peng Cui − *Department of Chemistry and Materials Innovation Factory, University of Liverpool, Liverpool L7 3NY, United Kingdom*

Complete contact information is available at: https://pubs.acs.org/10.1021/jacs.0c07732

Notes

The authors declare no competing financial interest.

ACKNOWLEDGMENTS

For funding, the authors acknowledge the Engineering and Physical Sciences Research Council (EPSRC) (EP/N004884/1) and the Leverhulme Trust via the Leverhulme Research Centre for Functional Materials Design. The authors acknowledge Diamond Light Source for access to beamlines I19 (CY21726) and I11 (CY23666). We thank Dr. A. Ken Inge and Mr. Erik Svensson Grape at the University of Stockholm for attempting to collect electron diffraction data for **3D-CageCOF-1**. We thank Dr. Michael E. Briggs and Prof. Jeffrey L. Katz for useful discussions related to the synthesis of **Cage-6-NH$_2$**. We thank Prof. Rochus Schmid for providing the weaver code; Mr. Xiaowei Zhu for help preparing the figures; and Dr. Luca Catalona for help performing DSC.

REFERENCES

(1) Cote, A. P.; Benin, A. I.; Ockwig, N. W.; O'Keeffe, M.; Matzger, A. J.; Yaghi, O. M. Porous, Crystalline, Covalent Organic Frameworks. *Science* **2005**, *310*, 1166−1170.

(2) El-Kaderi, H. M.; Hunt, J. R.; Mendoza-Cortes, J. L.; Cote, A. P.; Taylor, R. E.; O'Keeffe, M.; Yaghi, O. M. Designed Synthesis of 3D Covalent Organic Frameworks. *Science* **2007**, *316*, 268−272.

(3) Geng, K.; He, T.; Liu, R.; Dalapati, S.; Tan, K. T.; Li, Z.; Tao, S.; Gong, Y.; Jiang, Q.; Jiang, D. Covalent Organic Frameworks: Design, Synthesis, and Functions. *Chem. Rev.* **2020**, *120*, 8814.

(4) Guan, X.; Chen, F.; Fang, Q.; Qiu, S. Design and Applications of Three Dimensional Covalent Organic Frameworks. *Chem. Soc. Rev.* **2020**, *49*, 1357−1384.

(5) Yaghi, O. M.; O'Keeffe, M.; Ockwig, N. W.; Chae, H. K.; Eddaoudi, M.; Kim, J. Reticular Synthesis and the Design of New Materials. *Nature* **2003**, *423*, 705−714.

(6) Furukawa, H.; Cordova, K. E.; O'Keeffe, M.; Yaghi, O. M. The Chemistry and Applications of Metal-Organic Frameworks. *Science* **2013**, *341*, 1230444.

(7) Ma, X.; Scott, T. F. Approaches and Challenges in the Synthesis of Three-Dimensional Covalent-Organic Frameworks. *Commun. Chem.* **2018**, *1*, 98.

(8) Beuerle, F.; Gole, B. Covalent Organic Frameworks and Cage Compounds: Design and Applications of Polymeric and Discrete Organic Scaffolds. *Angew. Chem., Int. Ed.* **2018**, *57*, 4850−4878.

(9) O'Keeffe, M.; Peskov, M. A.; Ramsden, S. J.; Yaghi, O. M. The Reticular Chemistry Structure Resource (RCSR) Database of, and Symbols for, Crystal Nets. *Acc. Chem. Res.* **2008**, *41*, 1782−1789.

(10) Uribe-Romo, F. J.; Hunt, J. R.; Furukawa, H.; Klock, C.; O'Keeffe, M.; Yaghi, O. M. A Crystalline Imine-Linked 3-D Porous Covalent Organic Framework. *J. Am. Chem. Soc.* **2009**, *131*, 4570−4571.

(11) Ma, T.; Kapustin, E. A.; Yin, S. X.; Liang, L.; Zhou, Z.; Niu, J.; Li, L.-H.; Wang, Y.; Su, J.; Li, J.; Wang, X.; Wang, W. D.; Wang, W.; Sun, J.; Yaghi, O. M. Single-Crystal X-ray Diffraction Structures of Covalent Organic Frameworks. *Science* **2018**, *361*, 48−52.

(12) Lin, G.; Ding, H.; Yuan, D.; Wang, B.; Wang, C. A Pyrene-Based, Fluorescent Three-Dimensional Covalent Organic Framework. *J. Am. Chem. Soc.* **2016**, *138*, 3302−3305.
(13) Zhang, Y.; Duan, J.; Ma, D.; Li, P.; Li, S.; Li, H.; Zhou, J.; Ma, X.; Feng, X.; Wang, B. Three-Dimensional Anionic Cyclodextrin-Based Covalent Organic Frameworks. *Angew. Chem., Int. Ed.* **2017**, *56*, 16313−16317.
(14) Yahiaoui, O.; Fitch, A. N.; Hoffmann, F.; Froba, M.; Thomas, A.; Roeser, J. 3D Anionic Silicate Covalent Organic Framework with srs Topology. *J. Am. Chem. Soc.* **2018**, *140*, 5330−5333.
(15) Lan, Y.; Han, X.; Tong, M.; Huang, H.; Yang, Q.; Liu, D.; Zhao, X.; Zhong, C. Materials Genomics Methods for High-Throughput Construction of COFs and Targeted Synthesis. *Nat. Commun.* **2018**, *9*, 5274.
(16) Chen, Z.; Jiang, H.; Li, M.; O'Keeffe, M.; Eddaoudi, M. Reticular Chemistry 3.2: Typical Minimal Edge-Transitive Derived and Related Nets for the Design and Synthesis of Metal-Organic Frameworks. *Chem. Rev.* **2020**, *120*, 8039.
(17) Du, D. Y.; Qin, J. S.; Sun, Z.; Yan, L. K.; O'Keeffe, M.; Su, Z. M.; Li, S. L.; Wang, X. H.; Wang, X. L.; Lan, Y. Q. An Unprecedented (3,4,24)-Connected Heteropolyoxozincate Organic Framework as Heterogeneous Crystalline Lewis Acid Catalyst for Biodiesel Production. *Sci. Rep.* **2013**, *3*, 2616.
(18) Guillerm, V.; Kim, D.; Eubank, J. F.; Luebke, R.; Liu, X.; Adil, K.; Lah, M. S.; Eddaoudi, M. A Supermolecular Building Approachfor the Design and Construction of Metal−Organic Frameworks. *Chem. Soc. Rev.* **2014**, *43*, 6141−6172.
(19) Wright, P. A. *Microporous Framework Solids*; Royal Society of Chemistry: Cambridge, 2008.
(20) Li, M.; Li, D.; O'Keeffe, M.; Yaghi, O. M. Topological Analysis of Metal-Organic Frameworks with Polytopic Linkers and/or Multiple Building Units and the Minimal Transitivity Principle. *Chem. Rev.* **2014**, *114*, 1343−1370.
(21) Lee, J. M.; Cooper, A. I. Advances in Conjugated Microporous Polymers. *Chem. Rev.* **2020**, *120*, 2171−2214.
(22) Zhang, X.; Lin, R. B.; Wang, J.; Wang, B.; Liang, B.; Yildirim, T.; Zhang, J.; Zhou, W.; Chen, B. Optimization of the Pore Structures of MOFs for Record High Hydrogen Volumetric Working Capacity. *Adv. Mater.* **2020**, *32*, 1907995.
(23) Li, H.; Chang, J.; Li, S.; Guan, X.; Li, D.; Li, C.; Tang, L.; Xue, M.; Yan, Y.; Valtchev, V.; Qiu, S.; Fang, Q. Three-Dimensional Tetrathiafulvalene-Based Covalent Organic Frameworks for Tunable Electrical Conductivity. *J. Am. Chem. Soc.* **2019**, *141*, 13324−13329.
(24) Durholt, J. P.; Jahromi, B. F.; Schmid, R. Tuning the Electric Field Response of MOFs by Rotatable Dipolar Linkers. *ACS Cent. Sci.* **2019**, *5*, 1440−1448.
(25) Song, B. Q.; Yang, Q. Y.; Wang, S. Q.; Vandichel, M.; Kumar, A.; Crowley, C.; Kumar, N.; Deng, C. H.; GasconPerez, V.; Lusi, M.; Wu, H.; Zhou, W.; Zaworotko, M. J. Reversible Switching between Nonporous and Porous Phases of a New SIFSIX Coordination Network Induced by a Flexible Linker Ligand. *J. Am. Chem. Soc.* **2020**, *142*, 6896−6901.
(26) Chen, Y.; Shi, Z. L.; Wei, L.; Zhou, B.; Tan, J.; Zhou, H. L.; Zhang, Y. B. Guest-Dependent Dynamics in a 3D Covalent Organic Framework. *J. Am. Chem. Soc.* **2019**, *141*, 3298−3303.
(27) Ma, Y. X.; Li, Z. J.; Wei, L.; Ding, S. Y.; Zhang, Y. B.; Wang, W. A Dynamic Three-Dimensional Covalent Organic Framework. *J. Am. Chem. Soc.* **2017**, *139*, 4995−4998.
(28) Horike, S.; Shimomura, S.; Kitagawa, S. Soft porous crystals. *Nat. Chem.* **2009**, *1*, 695−704.
(29) Horcajada, P.; Serre, C.; Maurin, G.; Ramsahye, N. A.; Balas, F.; Vallet-Regi, M.; Sebban, M.; Taulelle, F.; Férey, G. Flexible Porous Metal-Organic Frameworks for a Controlled Drug Delivery. *J. Am. Chem. Soc.* **2008**, *130*, 6774−6780.
(30) Santolini, V.; Miklitz, M.; Berardo, E.; Jelfs, K. E. Topological Landscapes of Porous Organic Cages. *Nanoscale* **2017**, *9*, 5280−5298.
(31) Swamy, S. I.; Bacsa, J.; Jones, J. T. A.; Stylianou, K. C.; Steiner, A.; Ritchie, L. K.; Hasell, T.; Gould, J. A.; Laybourn, A.; Khimyak, Y. Z.; Adams, D. J.; Rosseinsky, M. J.; Cooper, A. I. A Metal-Organic Framework with a Covalently Prefabricated Porous Organic Linker. *J. Am. Chem. Soc.* **2010**, *132*, 12773−12775.
(32) Culshaw, J. L.; Cheng, G.; Schmidtmann, M.; Hasell, T.; Liu, M.; Adams, D. J.; Cooper, A. I. Dodecaamide Cages: Organic 12-arm Building Blocks for Supramolecular Chemistry. *J. Am. Chem. Soc.* **2013**, *135*, 10007−10010.
(33) Zhang, G.; Mastalerz, M. Organic Cage Compounds-From Shape-Persistency to Function. *Chem. Soc. Rev.* **2014**, *43*, 1934−1947.
(34) Ma, J. X.; Li, J.; Chen, Y. F.; Ning, R.; Ao, Y. F.; Liu, J. M.; Sun, J.; Wang, D. X.; Wang, Q. Q. Cage Based Crystalline Covalent Organic Frameworks. *J. Am. Chem. Soc.* **2019**, *141*, 3843−3848.
(35) Sudik, A. C.; Cote, A. P.; Yaghi, O. M. Metal-Organic Frameworks Based on Trigonal Prismatic Building Blocks and the New ″acs″ Topology. *Inorg. Chem.* **2005**, *44*, 2998−3000.
(36) Chen, Z.; Li, P.; Anderson, R.; Wang, X.; Zhang, X.; Robison, L.; Redfern, L. R.; Moribe, S.; Islamoglu, T.; Gómez-Gualdrón, D. A.; Yildirim, T.; Stoddart, J. F.; Farha, O. K. Balancing Volumetric and Gravimetric Uptake in Highly Porous Materials for Clean Energy. *Science* **2020**, *368*, 297−303.
(37) Schoedel, A.; Zaworotko, M. J. $[M_3(\mu_3\text{-}O)(O_2CR)_6]$ and Related Trigonal Prisms: Versatile Molecular Building Blocks for Crystal Engineering of Metal−Organic Material Platforms. *Chem. Sci.* **2014**, *5*, 1269−1282.
(38) Chen, Z.; Li, P.; Zhang, X.; Li, P.; Wasson, M. C.; Islamoglu, T.; Stoddart, J. F.; Farha, O. K. Reticular Access to Highly Porous acs-MOFs with Rigid Trigonal Prismatic Linkers for Water Sorption. *J. Am. Chem. Soc.* **2019**, *141*, 2900−2905.
(39) Katz, J. L.; Selby, K. J.; Conry, R. R. A Single-Step Synthesis of D_{3h}-Symmetric Bicyclooxacalixarenes. *Org. Lett.* **2005**, *7*, 3505−3507.
(40) Kalmutzki, M. J.; Hanikel, N.; Yaghi, O. M. Secondary Building Units as the Turning Point in the Development of the Reticular Chemistry of MOFs. *Sci. Adv.* **2018**, *4*, eaat9180.
(41) Kandambeth, S.; Shinde, D. B.; Panda, M. K.; Lukose, B.; Heine, T.; Banerjee, R. Enhancement of Chemical Stability and Crystallinity in Porphyrin-Containing Covalent Organic Frameworks by Intramolecular Hydrogen Bonds. *Angew. Chem., Int. Ed.* **2013**, *52*, 13052−10356.
(42) Keupp, J.; Schmid, R. TopoFF: MOF Structure Prediction Using Specifically Optimized Blueprints. *Faraday Discuss.* **2018**, *211*, 79−101.
(43) Guan, X.; Ma, Y.; Li, H.; Yusran, Y.; Xue, M.; Fang, Q.; Yan, Y.; Valtchev, V.; Qiu, S. Fast, Ambient Temperature and Pressure Ionothermal Synthesis of Three-Dimensional Covalent Organic Frameworks. *J. Am. Chem. Soc.* **2018**, *140*, 4494−4498.
(44) Lee, J. H.; Jeoung, S.; Chung, Y. G.; Moon, H. R. Elucidation of Flexible Metal-Organic Frameworks: Research Progresses and Recent Developments. *Coord. Chem. Rev.* **2019**, *389*, 161−188.
(45) Peh, S. B.; Karmakar, A.; Zhao, D. Multiscale Design of Flexible Metal−Organic Frameworks. *Trends in Chemistry* **2020**, *2*, 199−213.
(46) Yanai, N.; Kitayama, K.; Hijikata, Y.; Sato, H.; Matsuda, R.; Kubota, Y.; Takata, M.; Mizuno, M.; Uemura, T.; Kitagawa, S. Gas detection by structural variations of fluorescent guest molecules in a flexible porous coordination polymer. *Nat. Mater.* **2011**, *10*, 787−793.
(47) Wang, H.; Li, B.; Wu, H.; Hu, T. L.; Yao, Z.; Zhou, W.; Xiang, S.; Chen, B. A Flexible Microporous Hydrogen-Bonded Organic Framework for Gas Sorption and Separation. *J. Am. Chem. Soc.* **2015**, *137*, 9963−9970.
(48) Choi, H. S.; Suh, M. P. Highly Selective CO_2 Capture in Flexible 3D Coordination Polymer Networks. *Angew. Chem., Int. Ed.* **2009**, *48*, 6865−6869.
(49) Ozdemir, J.; Mosleh, I.; Abolhassani, M.; Greenlee, L. F.; Beitle, R. R.; Beyzavi, M. H. Covalent Organic Frameworks for the Capture, Fixation, or Reduction of CO_2. *Front. Energy Res.* **2019**, *7*, 77.
(50) Li, H.; Pan, Q.; Ma, Y.; Guan, X.; Xue, M.; Fang, Q.; Yan, Y.; Valtchev, V.; Qiu, S. Three-Dimensional Covalent Organic Frameworks with Dual Linkages for Bifunctional Cascade Catalysis. *J. Am. Chem. Soc.* **2016**, *138*, 14783−14788.
(51) Gao, Q.; Li, X.; Ning, G.-H.; Xu, H.-S.; Liu, C.; Tian, B.; Tang, W.; Loh, K. P. Covalent Organic Framework with Frustrated Bonding

Network for Enhanced Carbon Dioxide Storage. *Chem. Mater.* **2018**, *30*, 1762−1768.
(52) Nguyen, H. L.; Hanikel, N.; Lyle, S. J.; Zhu, C.; Proserpio, D. M.; Yaghi, O. M. A Porous Covalent Organic Framework with Voided Square Grid Topology for Atmospheric Water Harvesting. *J. Am. Chem. Soc.* **2020**, *142*, 2218−2221.

https://dx.doi.org/10.1021/jacs.0c07732
J. Am. Chem. Soc. 2020, 142, 16842−16848